Supplemental material to this article can be found at:
http://jpet.aspetjournals.org/content/suppl/2019/03/20/jpet.118.254755.DC1

1521-0103/369/3/503–510$35.00 https://doi.org/10.1124/jpet.118.254755
THE JOURNAL OF PHARMACOLOGY AND EXPERIMENTAL THERAPEUTICS J Pharmacol Exp Ther 369:503–510, June 2019




# CXA-10, a Nitrated Fatty Acid, Is Renoprotective in Deoxycorticosterone Acetate-Salt Nephropathy[S]

Cynthia M. Arbeeny, Hong Ling, Mandy M. Smith, Stephen O'Brien, Stefan Wawersik, Steven R. Ledbetter, Allen McAlexander, Francisco J. Schopfer, Robert N. Willette, and Diane K. Jorkasky

*Sanofi, Framingham (C.M.A., M.M.S., S.R.L.), Novartis (H.L., S.O.) and Scholar Rock (S.W.), Cambridge, Massachusetts; University of Pittsburgh, Pittsburgh, Pennsylvania (F.J.S) and Complexa, Inc., Berwyn, Pennsylvania (A.M., R.N.W., D.K.J.)*

Received October 31, 2018; accepted January 18, 2019

## ABSTRACT

Underlying pathogenic mechanisms in chronic kidney disease (CKD) include chronic inflammation, oxidant stress, and matrix remodeling associated with dysregulated nuclear factor-κ B, nuclear factor-κ B, and SMAD signaling pathways, respectively. Important cytoprotective mechanisms activated by oxidative inflammatory conditions are mediated by nitrated fatty acids that covalently modify proteins to limit inflammation and oxidant stress. In the present study, we evaluated the effects of chronic treatment with CXA-10 (10-nitro-9(E)-octadec-9-enoic acid) in the uninephrectomized deoxycorticosterone acetate–high-salt mouse model of CKD. After 4 weeks of treatment, CXA-10 [2.5 millligrams per kilogram (mpk), p.o.] significantly attenuated increases in plasma cholesterol, heart weight, and kidney weight observed in the model without impacting systemic arterial blood pressure. CXA-10 also reduced albuminuria, nephrinuria, glomerular hypertrophy, and glomerulosclerosis in the model. Inflammatory MCP-1 and fibrosis (collagen, fibronectin, plasminogen activator inhibitor-1, and osteopontin) renal biomarkers were significantly reduced in the CXA-10 (2.5 mpk) group. The anti-inflammatory and antifibrotic effects, as well as glomerular protection, were not observed in the enalapril-treated group. Also, CXA-10 appears to exhibit hormesis as all protective effects observed in the low-dose group were absent in the high-dose group (12.5 mpk). Taken together, these findings demonstrate that, at the appropriate dose, the nitrated fatty acid CXA-10 exhibits anti-inflammatory and antifibrotic effects in the kidney and limits renal injury in a model of CKD.

## Introduction

Chronic kidney disease (CKD), the primary cause of end-stage renal disease, is expected to exceed 50 million individuals in the United States by 2025. Because of its negative effect on the progression of other prevalent comorbidities, CKD will have a large impact on overall health status and health care costs, highlighting the urgent need for effective new therapies (Hoerger et al., 2015).

Whether primary, secondary, idiopathic, or heritable, all forms of CKD ultimately affect vascular, glomerular, tubular, and matrix components of the kidney. The major underlying pathogenic mechanisms identified to date include chronic inflammation, oxidant stress, and matrix remodeling associated with dysregulated NF-κB, NRF2, and SMAD signaling pathways, respectively. Important cytoprotective mechanisms are also activated endogenously by oxidative inflammatory conditions and include the nonenzymatic generation of nitrated fatty acids ($NO_2$-FA) derived from unsaturated fatty acids and free radical oxides of nitrogen [nitric oxide (NO)-derivatives]. $NO_2$-FAs are electrophilic fatty acids that mediate reversible Michael addition reactions with cellular nucleophiles, such as cysteine- and histidine-containing proteins, to regulate their structure and function. These posttranslational modifications of a selective redox-sensitive pool of proteins impact key adaptive signaling pathways to limit inflammation, oxidant stress, and excessive matrix production (Delmastro-Greenwood et al., 2014; Villacorta et al., 2016).

CXA-10 (10-nitro-9(E)-octadec-9-enoic acid) is a naturally occurring $NO_2$-FA formulated for oral and intravenous administration that is currently in clinical development for renal and pulmonary indications (Schopfer et al., 2018). Specific molecular interactions that contribute to the pharmacologic actions of CXA-10 include the following: 1) the adduction of key cysteine residues (Cys273 and 288) of Keap1, the nuclear factor (erythroid-derived 2)-like 2 (NRF2) inhibitor, that releases NRF2 to activate the antioxidant response element (ARE) pathway to upregulate antioxidant and detoxifying

All studies were supported by Sanofi Genzyme, Framingham, MA.
https://doi.org/10.1124/jpet.118.254755.
[S]This article has supplemental material available at jpet.aspetjournals.org.

**ABBREVIATIONS:** ARE, antioxidant response element; CKD, chronic kidney disease; CXA-10, (10-nitro-9(E)-octadec-9-enoic acid); DOCA, deoxycorticosterone acetate; ELISA, enzyme-linked immunosorbent assay; GFR, glomerular filtratin rate; MCP-1, monocyte chemotractant protein-1; mpk, milligrams per kilogram; NF-kB, nuclear factor-κ B; NO, nitric oxide; $NO_2$-FA, nitrated fatty acid; NRF2, nuclear factor (erythroid-derived 2)-like 2; PAI-1, plasminogen activator inhibitor-1; PCR, polymerase chain reaction; SMAD, small, mothers against decapentaplegic; Unx, uninephrectomized; WT-1, Wilms tumor 1.

protein production; 2) the adduction of a cysteine residue (Cys38) of the p65 subunit of nuclear factor κ-light-chain-enhancer of activated B cells (NF-κB), which disrupts the TLR4 signaling complex and prevents elaboration of proinflammatory and profibrotic mediators; 3) binding to heat shock response elements and driving expression of heat shock proteins, which act as chaperons during cellular stress; and 4) inhibition of xanthine oxidoreductase, one of the major enzymes involved in the production of reactive oxygen species (Cui et al., 2006; Kelley et al., 2008; Kansanen et al., 2009, 2011; Villacorta et al., 2013, 2016).

In the present study, we compared the effects of low and high oral dose treatments of CXA-10 with enalapril treatment in the low renin deoxycorticosterone acetate (DOCA)-high-salt mouse model of CKD. All treatments were started 4 weeks after uninephrectomy (Unx) and 2 weeks after initiating DOCA-high salt administration at a time when CKD was evident and progressing. Circulatory, metabolic, and renal parameters were assessed after 4 weeks of treatment.

## Materials and Methods

**DOCA Mouse Model and Study Design.** Male mice (129/sv strain) were purchased from Taconic Biosciences (Hudson, NY). The animals underwent Unx at 6 weeks of age by the vendor and were shipped 1 week after surgery. Two weeks after Unx, a DOCA or placebo pellet (21-day-release pellets, 50 mg/pellet; Innovative Research of America, Sarasota, FL) was implanted subcutaneously. All mice were then placed on a semisynthetic diet that contained a moderate fat content and a low phytoestrogen/antioxidant level, which approximates a normal human diet (4). A second DOCA or placebo pellet was implanted 3 weeks later.

All animal studies complied with the Guide for the Care and Use of Laboratory Animals as published by the US National Institutes of Health and were approved by the Institutional Animal Care and Use Committee at Sanofi (Framingham, MA).

**Treatment.** Mice were treated with vehicle (sesame oil), CXA-10 at a dose of 2.5 and 12.5 mg/kg (oral gavage, once daily), or enalapril (20 mpk per day in drinking water), as indicated in Fig. 1, for 4 weeks, starting 2 weeks after the first DOCA pellet implantation. Each group of mice except the sham control group had ab libitum access to a 1% NaCl solution in tap water for the duration of the study. Body weight was measured weekly, and all doses were adjusted accordingly. Urine and blood samples were collected before treatment and at weeks 2 and 4 of treatment. All data are presented as the mean ± S.E.M. for the number of animals listed in each group. The study design and timeline are shown in Fig. 1.

**Serum and Urine Analyses.** We performed blood sample extraction from retro-orbital sinus and isolated serum using standard methods. We analyzed serum and urine creatinine (enzymatic assay), blood urea nitrogen, and serum cholesterol using a Cobas 400 plus bioanalyzer (Roche Diagnostics, Indianapolis, IN). Urine samples were collected for 24 hours using metabolic cages. Urine albumin was measured by immunoassay Albuwell M (Exocell Inc., Philadelphia, PA). Immuno-enzyme-linked immunosorbent assay (ELISA) according to manufacturer's instructions was used to measure urine nephrin (Exocell Inc.) and MCP-1 (Thermal Scientific, Waltham, MA). KIM-1 (Kidney Injury Marker -1) was measured using the E-90KIM mouse ELISA kit (Immunology Consultants Laboratory, Portland, OR).

**Glomerular Filtration Rate.** Glomerular filtration rate (GFR) was measured at the 4-week timepoint using a FIT-GFR test kit for inulin according to manufacturer's instructions (BioPal, Worcester, MA). A 5-mkg bolus intraperitoneal injection of inulin was administered, followed by serial saphenous bleeds at 30, 60, and 90 minutes. Serum inulin was quantified by an inulin ELISA. Inulin serum clearance was determined by nonlinear regression using a one-phase exponential decay formula according to the manufacturer's instructions.

**Histologic Assessment.** We stained 3-μm-thin sections of formalin-fixed, paraffin-embedded kidneys with H&E, periodic acid-Schiff, picro-sirius red, and Masson's trichrome for histologic analysis. Slides were blindly evaluated by an experienced pathology investigator. Glomerular and tubular pathology, interstitial inflammation, and interstitial fibrosis were semiquantitatively scored on a scale of 0–4 as follows: 0 = normal, 1 = mild, 2 = moderate, 3 = marked, 4 = severe.

**Immunohistochemistry.** Podocyte numbers were assessed using anti-WT1 (Wilms tumor 1) clone 6F-H2 at 1:100 dilution (Dako, Carpinteria, CA). Immunohistochemistry was performed on a Leica Bond MAX automated immunostaining instrument (Leica Microsystems Inc., Bannockburn, IL). A 0.05% Tween20/Tris-buffered saline (Dako) solution wash was performed between all steps. Tissue sections were dewaxed, treated with proteinase K enzyme, and then peroxidase. Tissues were then treated with rodent blocking agent (BioGenex, Fremont, CA) and incubated with anti-WT-1 primary antibody (clone 6F-H2, 1:100; Dako), which was then detected using a streptavidin-horseradish peroxidase-conjugated secondary mouse anti-mouse antibody. Chromagen visualization was performed using 3,3′-diaminobenzidine tetrahydrochloride for 5 minutes, followed by hematoxylin counterstain and dehydration through increasing ethanol-water gradient to xylene, and mounted in Permount (Fisher Scientific, Pittsburg, PA). Whole-kidney sections were imaged using



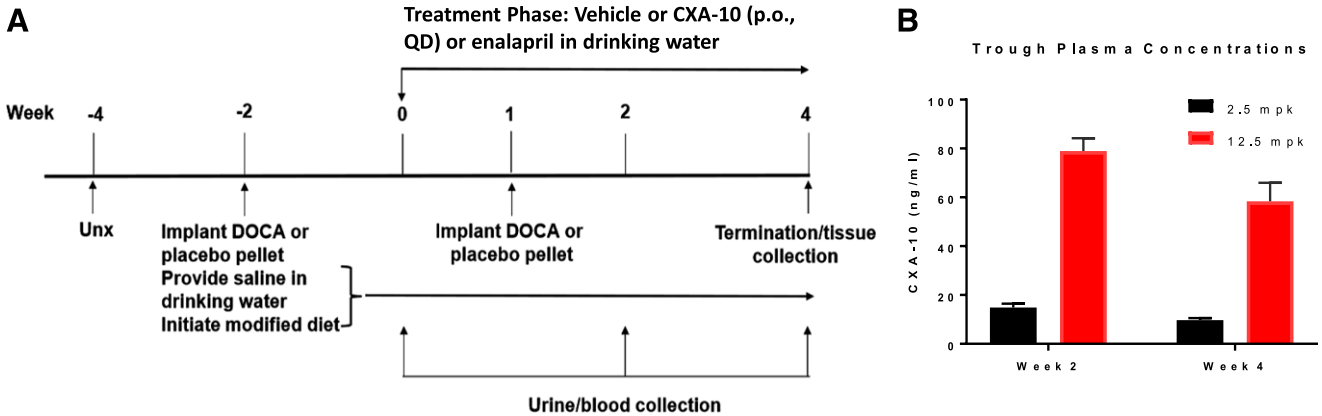


**Fig. 1.** Study design and timeline (A). Treatment details and procedures are described in the *Materials and Methods* section. Unx was performed 2 weeks before starting the DOCA/salt regimen and 4 weeks before treatments. Vehicle (sesame oil) and CXA-10 were administered by daily oral gavage. Mean trough plasma concentrations of CXA-10 (±S.E.M.) for the low- and high-dose groups of CXA-10 were determined after 2 and 4 weeks of treatment (B).

Aperio ScanScope (Aperio Technologies, Vista, CA). Fifty glomeruli per kidney section were quantitated for the number of WT-1-positive (brown) and WT-1-negative cells (blue). Software analysis was performed using a custom algorithm on Spectrum Version 11.0.0.725 (Aperio Technologies). Immunohistochemistry was also performed to examine CD31 (Abcam, Cambridge, MA), a marker of endothelial integrity.

**Reverse Transcription-Polymerase Chain Reaction Analysis of Gene Expression.** A portion of kidney from each mouse was snap-frozen in Trizol solution (Invitrogen, Carlsbad, CA) immediately after harvesting and stored at −80°C until analysis. Tissues were homogenized using a bead mill in 0.5 ml of Trizol solution, and total RNA was extracted with chloroform (Sigma, St. Louis, MO) and purified using standard RNeasy mini kit (Qiagen, Germantown, MD), with on-column DNase 1 (Qiagen) digestion to avoid nonspecific fluorescence emission derived from the recognition of contaminating genomic DNA by the probe according to the manufacturer's recommendation. RNA samples were eluted in 30 $\mu$l of nuclease-free water and quantified using a Nanodrop (Thermo Fisher Scientific, Waltham, MA). cDNA was generated from 2 $\mu$g of RNA by using Clontech Sprint PowerScript reagents (Clontech Laboratories, Mountain View, CA) according to the manufacturer's protocol. Fluorogenic probes specific for genes assayed in the report were purchased from Applied Biosystems (Foster City, CA). PCR amplification and analysis of PCR reaction were performed and monitored using an ABI Prism 7900HT Sequence Detection System (TaqMan; PerkinElmer Applied Biosystems, Waltham, MA). Data analysis was carried out by using the Sequence Detection Systems v2.3 program (Applied Biosystems). For each cDNA sample, the cycle threshold value of each target sequence was normalized to reference gene (ribosomal RNA-18S) and shown as fold changes to control group.

**Statistical Analysis.** Statistical analyses for serum and urine data and gene expression data were performed using a two-tailed Student's $t$ test. Statistical analysis of the histologic data was performed using the nonparametric Kruskal-Wallis tes,t followed by Dunn's multiple comparison test.

## Results

**Systemic Effects and Pharmacokinetics.** Unx was associated with a slight reduction in body weight in both vehicle and treatment groups; however, body weight gains over the course of the study were unaffected by CXA-10 or enalapril treatments in the DOCA-salt groups (Fig. 2A). The addition of DOCA-salt caused a modest increase in mean arterial pressure (~20 mm Hg) in the model, which was not mitigated by any of the treatments, including enalapril, (Fig. 2B). Plasma total cholesterol levels were also significantly elevated by DOCA-salt in the vehicle group (>100%) and were reduced by either low-dose CXA-10 or enalapril (Fig. 2C). Kidney weight/body weight and heart weight/body weight ratios were increased by DOCA-salt administration in this model and were attenuated significantly by low-dose CXA-10 treatment (Fig. 2C). Enalapril had no effect on heart and kidney weights in this model. The enlarged kidneys in renal injury groups were unremarkable with no distinguishing gross features.

We administered CXA-10 after 2 and 4 weeks of oral daily treatment in the DOCA-salt model and determined

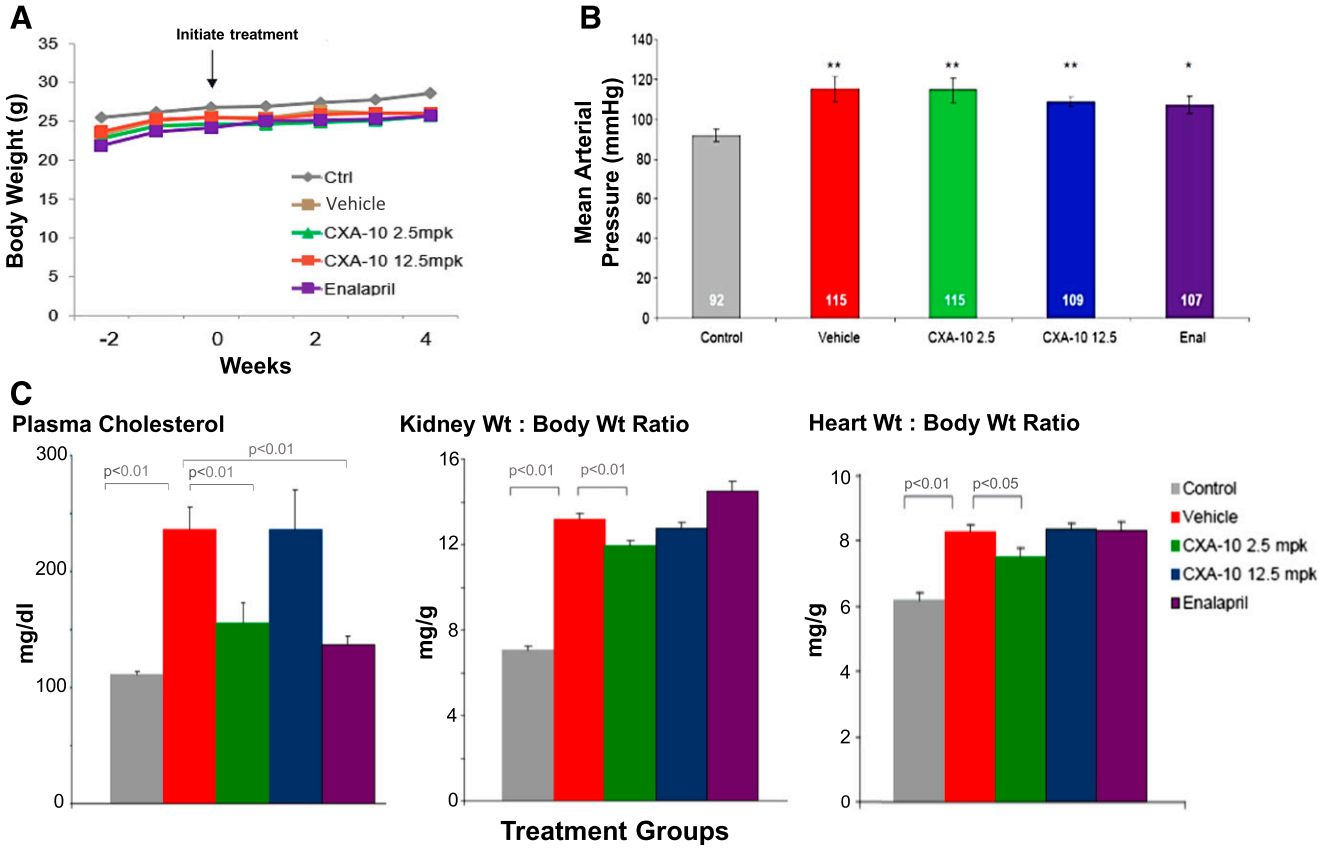


**Fig. 2.** The DOCA salt-fat diet regimen had significant systemic effects on body weight (A); mean arterial pressure (B); and plasma cholesterol, kidney weight, and heart weight (C) in the Unx mouse (vehicle vs. control). Treatment effects were evaluated at the end of the 4-week protocol. $^{**}P < 0.01$; $^{*}P < 0.05$ vs. vehicle. Treatment with the low dose of CXA-10 significantly reduced plasma cholesterol, kidney weight/body weight ratio, and heart weight/body weight relative to the vehicle treated group.

trough (23 hours after the final dose) plasma concentrations of CXA-10 by liquid chromatography-mass spectrometry. The average plasma concentrations of CXA-10 for the low-dose (2.5 mg/kg) group at 2 and 4 weeks were 14.9 and 9.7 ng/ml, respectively, and 79 and 58.4 ng/ml in the high dose (12.5 mg/kg) group (Fig. 1B). CXA-10 plasma levels were below the lower limit of quantification in all predose samples, indicating that endogenous levels of CXA-10 were undetectable and that exposures in the low- and high-dose groups were dose-proportional at each time point.

**Renal Effects.** The introduction of DOCA-salt in the model increased urinary albumin, nephrin, and KIM-1 excretion (Fig. 3; Supplemental Fig. 1). All active treatments reduced albuminuria at 2 weeks, but only low-dose CXA-10 (2.5 mg/kg) and enalapril were efficacious at 4 weeks (Fig. 3A; Supplemental Fig. 1). Elevated urinary nephrin, suggestive of podocyte injury, was also apparent at 2 and 4 weeks in the model (Fig. 3B). Treatment with low-dose CXA-10 reduced nephrinuria after 4 weeks, whereas enalapril was effective at both 2 and 4 weeks of treatment (Fig. 3B). Urinary KIM-1 excretion, a marker of tubular injury associated with regions of inflammation and fibrosis (Humphreys et al., 2013), was also increased by DOCA-salt administration in the model (Fig. 3C). There was an apparent trend to decrease urinary KIM-1 in both low-dose CXA-10 ($P < 0.1$) and enalapril groups ($P = 0.06$).

The DOCA-salt model caused a modest decrease in GFR, assessed using the inulin method, that did not reach statistical significance (Supplemental Fig. 2A); however, there was a trend toward an increased GFR in mice treated with enalapril. Consistent with the modest effects on GFR, serum creatinine and blood urea nitrogen remained within the normal range for all groups in this model (Supplemental Fig. 2, B and C).

**Histopathologv and Immunohistochemical Analysis.** The introduction of DOCA-salt caused histopathologic changes in tubules and glomeruli. In the vehicle-treated DOCA group, approximately 15% of glomeruli displayed mild to severe glomerular damage, including mesangial expansion and sclerosis (see Fig. 4A for representative images). Tubular damage was also evident, showing patchy lesions of dilated tubules, casts, and tubulointerstitial expansion and fibrosis. After 4 weeks of treatment, tubulointerstitial lesions were improved in mice receiving enalapril or low-dose CXA-10, but only slightly with the high dose. Glomerulosclerosis was assessed and scored individually on a 1–4 ascending severity scale (Fig. 4B). Average injury scores and percentage of glomerular damage (sclerosis) were significantly reduced with both doses of CXA-10 but were not significantly altered by enalapril treatment (Fig. 4C).

Glomerular hypertrophy, a marker known to be associated with diabetic and hypertensive chronic kidney disease, was evaluated by measuring glomerular area, expressed as a mean value of 50 glomeruli per kidney. As expected, glomerular hypertrophy was evident in the vehicle treated group compared with sham control. The hypertrophic response was nearly abolished in the low-dose CXA-10 (2.5 mpk) group and was unaffected in the high-dose CXA-10 (12.5 mpk) and enalapril groups (Fig. 4B).

We quantified podocyte number by WT-1 immunostaining, which was unchanged in all treatment groups. Moreover, podocyte marker gene expression was not altered, suggesting a modest level of podocyte injury in this model (Supplemental Fig. 3).

Endothelial injury was assessed in renal tissue by performing immunohistochemistry staining to detect $CD31^+$ cells (Supplemental Fig. 4), which is a marker for endothelial integrity. CD31+ cell numbers were unchanged in all groups, consistent with a lack of obvious vasculopathy in the model.

**Inflammation, Fibrosis, and Oxidant Stress Biomarkers.** The chemokine MCP-1 is a key inflammatory mediator and biomarker of chronic kidney diseases (Vianna et al., 2013). In the DOCA-salt model, urinary MCP-1 excretion and renal *Mcp-1* gene expression were elevated at 4 weeks in the vehicle-treated group and were significantly reduced in mice treated with the low dose of CXA-10 for 4 weeks. The high dose of CXA-10 (12.5 mpk) and enalapril had no significant effect on MCP-1 excretion or expression (Fig. 5, A and B).

We evaluated gene expression of extracellular matrix biomarkers (osteopontin, collagen III, fibronectin and PAI-1) in mRNA extracted from whole-kidney lysates using quantitative reverse transcription-PCR. The results (Fig. 5C) indicate that gene expression of extracellular matrix remodeling mediators was significantly upregulated by DOCA-salt administration in vehicle-treated mice at 4 weeks. Treatment with low-dose CXA-10 attenuated the upregulation of these genes in the model; however, neither the high dose CXA-10 nor enalapril prevented the upregulation of these genes. These data are consistent with the histopathologic findings and support both anti-inflammatory and antifibrotic effects of CXA-10.



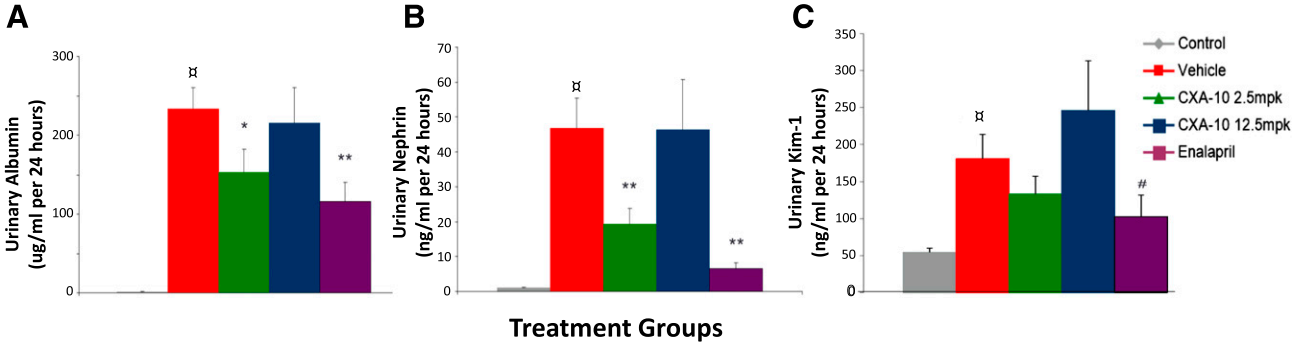


**Fig. 3.** The DOCA salt-fat diet regimen significantly increased urinary albumin (A), nephrin (B), and Kim-1 (C) excretion in the uninephrectomized mouse (¤$P < 0.01$, control vs. vehicle). Treatment effects were evaluated at the end of the 4-week protocol; **$P < 0.01$; *$P < 0.05$; $^{\#}P = 0.06$ vs. vehicle. Treatment with the low dose of CXA-10 or enalapril significantly decreased urinary albumin and nephrin relative to the vehicle-treated group.

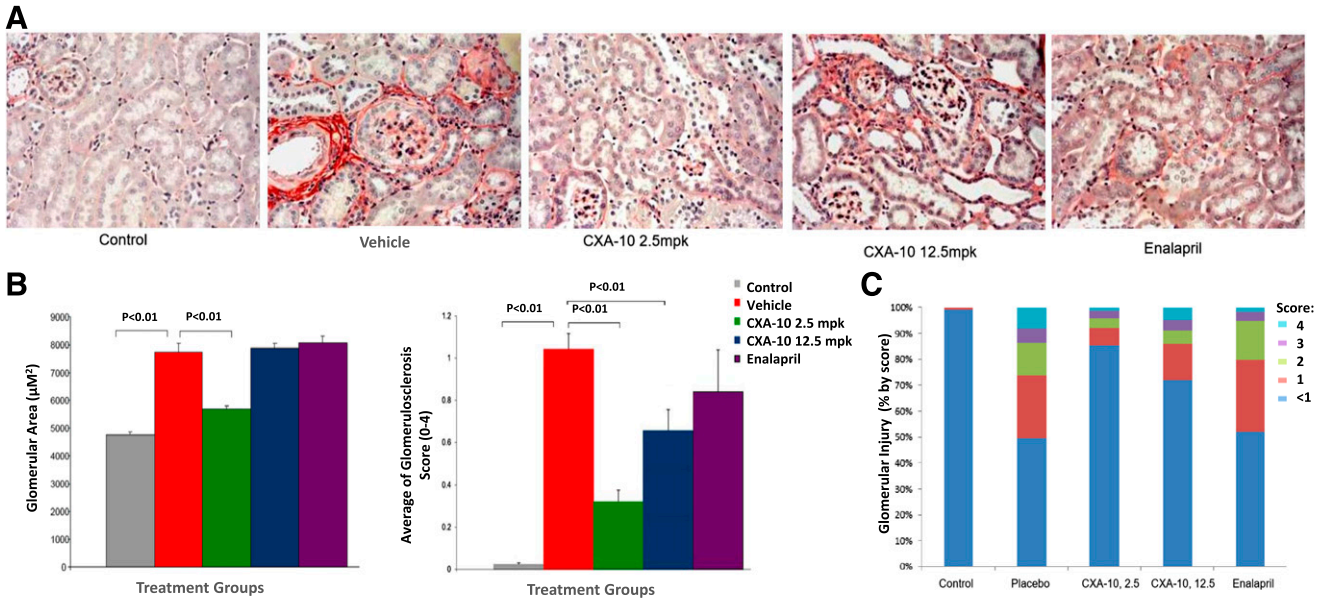


**Fig. 4.** Histologic evaluation of the Unx DOCA salt/fat model revealed mild to severe glomerular damage after 4 weeks [representative picro-sirius red photomicrographs in (A)] that included mesangial expansion and glomerulosclerosis (B and C). Treatment effects were quantified, scored, and compared statistically (B and C). Only CXA-10 abrogated the glomerular histopathology observed in this model.

Isoprostanes are a unique series of prostaglandin-like compounds formed in vivo via nonenzymatic mechanisms involving the free radical–initiated peroxidation of arachidonic acid. In the present study, we measured urinary 8-iso-PGF2a (the isoprostane that generally correlates best with increasing oxidant stress) and its urinary metabolite, tetranor-PGDM, using liquid chromatography-mass spectrometry at 2 and 4 weeks, but the marginal effects of DOCA-salt and highly variable isoprostane levels precluded any meaningful analysis of this data (data not shown).

## Discussion

CKD comprises a heterogenous group of diseases that manifest as prolonged and progressive renal dysfunction. Despite disparate causes, pathway analyses derived from CKD patient kidney biopsies and animal models revealed a common pattern of dysregulated metabolism, inflammation, and matrix remodeling and identified NRF2, an oxidant stress-regulated transcription factor, and NF-kB, a protein complex controlling inflammatory gene expression, as crucial pathogenic hubs (Grgic et al., 2014; Martini et al., 2014). NO2-FAs are key endogenous modulators of inflammation, oxidant stress, and fibrosis that serve as electrophiles, forming adducts with reactive cysteines in specific proteins to alter functionality. Both NF-kB and NRF2 complexes are known targets of NO2-FAs that are attenuated and activated by NO2-FAs, respectively. Transcriptional activation occurs by NO2-FA modification of Cys273 and 288 in Keap1 complexed to NRF2; this causes NRF2 liberation, nuclear translocation, binding to AREs, and increases in the expression of antioxidant and detoxifying proteins. NO2-FAs also form adducts at cysteine residues that regulate heat shock response elements and xanthine oxidoreductase to further limit inflammation, oxidant stress, and fibrosis (Kelley et al., 2008; Kansanen et al., 2009, 2011; Villacorta et al., 2013, 2016). For these reasons, we evaluated CXA-10 (10-nitro-9(E)-octadec-9-enoic acid), a naturally occurring $NO_2$-FA acid, in a low renin deoxycorticosterone acetate (DOCA)-high salt mouse model of CKD and compared its effects to enalapril. The findings suggest that CXA-10 (2.5 mg/kg, p.o daily, for 4 weeks) was renoprotective in the DOCA-high salt mouse model of CKD and exerted additional positive effects that were differentiated from enalapril treatment.

CXA-10 (2.5 mg/kg) and enalapril independently reduced the progression of both albuminuria and nephrinuria, suggesting improved podocyte filtration and/or proximal tubular protein reabsorption in this model. At 4 weeks, however, CXA-10 exceeded the ability of enalapril to reduce glomerular hypertrophy, glomerular injury score, and glomerulosclerosis index, as well as the overall kidney hypertrophy observed in the model. The gene expression of renal MCP-1, *Col3a1* procollagen type III, fibronectin, osteopontin, and PAI-1 showed a similar response pattern when comparing CXA-10 and enalapril, suggesting that the renoprotective mechanism of CXA-10 more directly involves modulation of chronic inflammation and active fibrosis. Of note, CXA-10 markedly decreased urinary MCP-1 excretion, an inflammatory mediator strongly associated with sustained renal decline in patients with type 2 diabetes (Nadkarni et al., 2016). In addition, the effects of CXA-10 were independent of obvious hemodynamic effects. The unique mechanisms engaged by CXA-10 versus enalapril are consistent with their combined additive renoprotective effects described in the db/db mouse model of diabetic nephropathy (Liu et al., 2013; Zoja et al., 2014). These results suggest that CXA-10 would address pathogenic mechanisms not impacted by current treatment and would be a complementary addition to the standard of care for CKD.

It is noteworthy that DOCA-salt hypertension in rats and mice is associated with dyslipidemia and liver steatosis, which are related to changes in metabolic enzyme activity rather than hyperphagia (Wang et al., 2015). In the present study, we

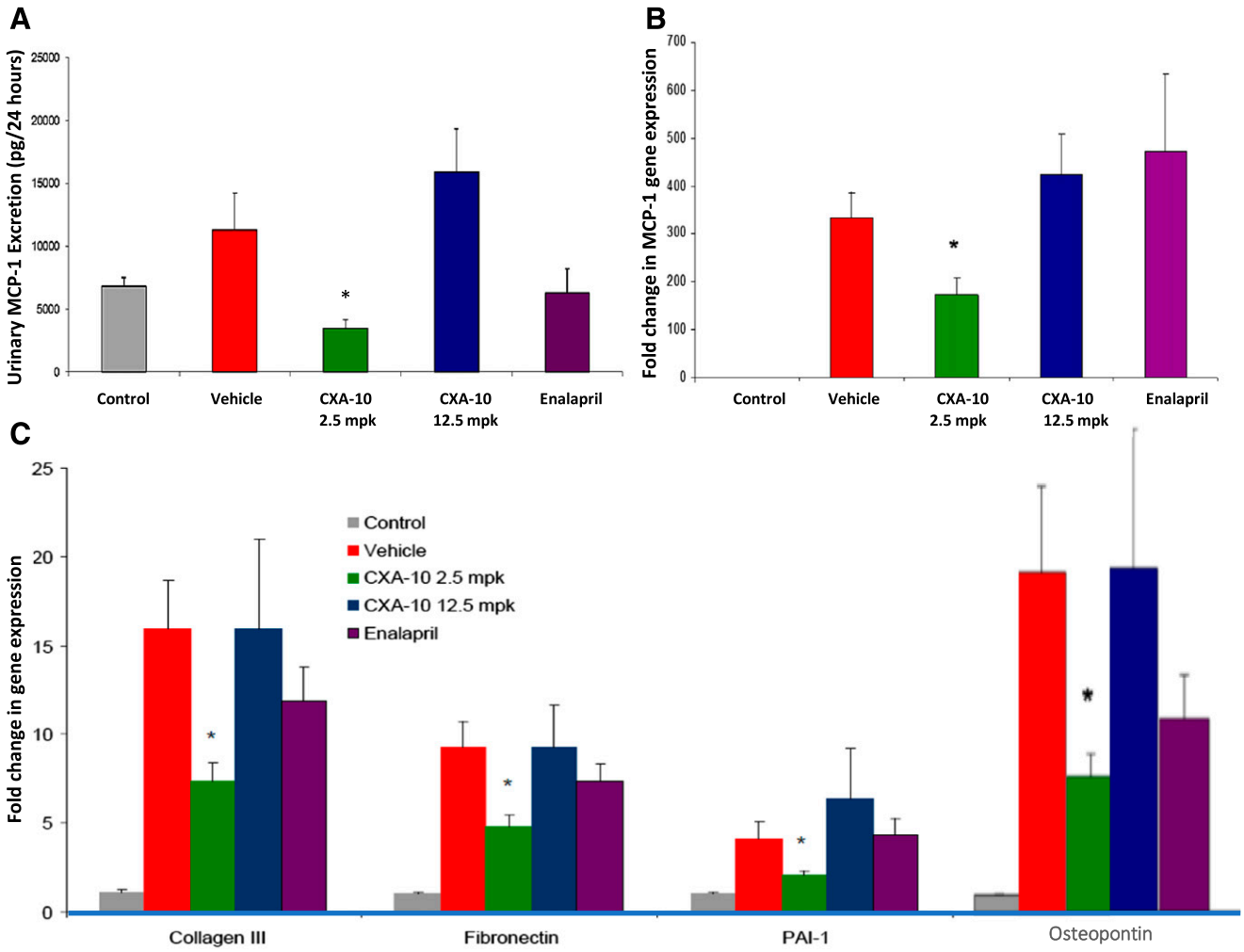


**Fig. 5.** The effects of treatment on inflammatory and fibrosis biomarkers were evaluated in the uninephrectomized DOCA salt-fat mouse model. Urinary MCP-1 excretion (A) and renal MCP-1 gene expression (B) were reduced significantly in the CXA-10 (2.5 mpk) group (*$P < 0.05$ vs. vehicle). Fibrosis-related genes (C), collagen III, fibronectin, PAI-1, and osteopontin were also reduced in the low-dose CXA-10 group ($P = 0.05$ vs. vehicle).

monitored the elevation of total plasma cholesterol as a marker of the DOCA-salt–induced metabolic disturbance. Both low-dose CXA-10 and enalapril markedly attenuated DOCA-salt hypercholesterolemia without altering body weight. The mechanisms underlying these protective metabolic effects are unknown but are consistent with the ability of electrophilic mediators, such as nitrated fatty acids, to act as endogenous ligands for peroxisome proliferator-activated receptors, which are known to have profound effects on lipid and glucose metabolism (Wang et al., 2010).

The DOCA-salt hypertension model also reliably exhibits left ventricular hypertrophy associated with reactivation of cardiac fetal gene expression, activation of growth and matrix pathways, increased protein synthesis, and increased interstitial and perivascular fibrosis (Kee et al., 2013). In the present study, the ratio of heart weight to body weight was increased >30% in vehicle treated mice. Consistent with the general pattern of end-organ protection, the low-dose CXA-10 treatment significantly attenuated cardiac hypertrophy without affecting systemic blood pressure. Enalapril and high-dose CXA-10 had no effect on cardiac hypertrophy. Detailed characterization of the hypertrophic response and the protective mechanism of CXA-10 was not performed in the current study, but antioxidant and anti-inflammatory targets of CXA-10 (e.g., NRF2 and NF-kB) are known to play a role in cardiac hypertrophy and fibrosis (Jadhav et al., 2008; Kee et al., 2013).

The protective effects of CXA-10 in this CKD model raise interesting questions not addressed in the current study. First, the precise cellular mechanisms underlying the effects of CXA-10 were not evaluated in the present study. A dedicated tissue flow cytometry study to evaluate effects on the macrophage may provide insight into the anti-inflammatory effects of CXA-10. Emerging evidence suggests that NRF-2 and nitro-fatty acids may have differential effects on proinflammatory and reparative macrophages (Kadl et al., 2010; Verescakova et al., 2017); however, a comprehensive evaluation of NRF-2 or nitro-fatty acid actions on the full complement of macrophage subtypes has not yet been reported. Second, although nitro-fatty acid activation of NRF2 antioxidant response genes is well documented (Wang et al., 2016; Schopfer et al., 2018), the precise genes and cell types and level of activation responsible for renal protection in this CKD model have not yet been defined. Double-labeling immunohistochemistry, laser capture dissection, and/or tissue flow cytometry may be useful in future for addressing these questions.

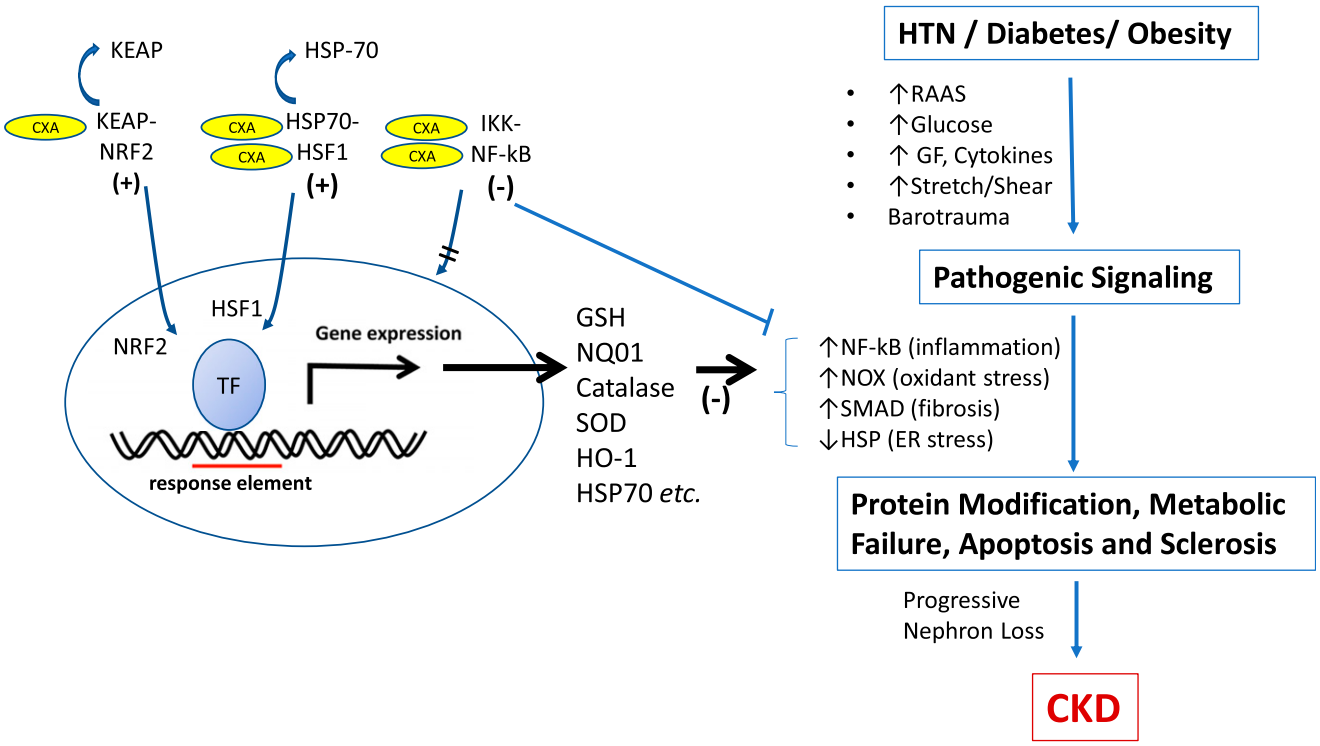


**Fig. 6.** This conceptual model illustrates pleiotropic cytoprotective effects of nitro-fatty acids (CXA-10) and how they would act to attenuate the progression of CKD. Post-translational modification of cytoplasmic proteins by CXA-10 facilitates gene expression by releasing complexed transcription factors (TF) such as NRF2 and HSF1, for nuclear translocation and interaction with their respective response elements and cofactors. Conversely, post-translational modification of cytoplasmic proteins by CXA-10 can also stabilize protein complexes and inhibit gene expression, as is the case with NFkB via IKK inhibition. Limiting inflammation, oxidant stress, and fibrosis by activating the antioxidant response pathway and the heat shock pathway, while inhibiting proinflammatory signaling through NFkB, would be expected to restore homeostasis in the kidney by countering pathogenic signaling driven by hypertension (HTN), diabetes, and/or obesity. GF, growth factors; GSH, reduced glutathione; HO-1, heme oxygenase 1; HSP70, 70-kilodalton heat shock protein; IKK, IκB kinase; KEAP, Kelch-like ECH-associated protein 1; NOX, NADPH oxidase; NQ01, NAD(P)H:quinone acceptor oxidoreductase 1; NRF2, nuclear factor (erythroid-derived 2)-like 2; RAAS, renin angiotensin aldosterone system; SOD, superoxide dismutase.

In stark contrast to the protective effects observed in the low-dose CXA-10 group, the high dose of CXA-10 (12.5 mg/kg, p.o., daily) exhibited only modest and transient renoprotective effects and had no effect on any of the markers of disease progression at the 4-week time point. The apparent loss of protection at the high dose is likely an example of an hormetic dose-response relationship mediated by the high levels of CXA-10 impacting NRF2-ARE and NF-kB pathways. These apparent hormetic responses have been reported previously for electrophilic NRF2 activators and inhibition of the NF-kB pathway (Calabrese, 2013; Bhakta-Guha and Efferth, 2015) in cellular assays, in preclinical animal models, and in humans. Like CXA-10, bardoxolone and sulforaphane electrophiles also exhibit hormetic dose-response curves in a variety of biologic systems (Maher and Yamamoto, 2010; Tan et al., 2014; Calabrese et al., 2016). Although we do not know the precise hormetic mechanism, it is conceivable that the pleiotropic electrophilic effects of nitro-fatty acids could, through post-translational protein modifications, activate a protective pathway at one dose and then have the opposite effect at a higher dose by subsequent downstream modifications to inactivate effector protein nucleophilic targets ("off-targets") that are less susceptible to adduction at lower electrophile concentrations. This mechanism of hormesis would not necessarily evoke toxicities and would be consistent observations in the current study (i.e., loss of effect without obvious toxicities, and with lack of hormesis on the primary antioxidant gene expression response) (Tan et al., 2014). "Downstream" hormetic targets may include cysteine residues in enzymes (metabolic, repair/defense, epigenetic), the antioxidant glutathiione, and/or membrane transporters. The hormesis observed in this study highlights the importance of a more thorough examination of the dose-response relationship in future studies.

Our current findings suggest that CXA-10 administered by the oral route can exert significant renoprotection and additional positive systemic effects in the DOCA-salt model of CKD without altering systemic arterial blood pressure. A conceptual model summarizing these actions and their effect on CKD progression is presented in Fig. 6. The evidence suggests that the protective mechanisms of CXA-10 are mediated by antioxidant, anti-inflammatory, and antifibrotic actions that can be differentiated from enalapril and are largely consistent with the established ability of NO2-FAs to inhibit and activate NF-kB and NRF2 signaling, respectively. Finally, the beneficial effects described herein support the clinical development of CXA-10 aimed at treating disorders associated with excessive oxidant stress, inflammation, and/or fibrosis.

#### Authorship Contributions

*Participated in research design:* Arbeeny, Jorkasky, Ledbetter.
*Conducted experiments:* Ling, Smith, O'Brien, Wawersik.
*Performed data analysis:* Arbeeny, Ledbdtter, Ling.
*Wrote or contributed to the writing of the manuscript:* Jorkasky, Ling, McAlexander, Willette.

***Note Added in Proof***—The 8th author Francisco J Schopfer was accidentally left off the Fast Forward version of the article published March 20, 2019. The author list and affiliation list has been corrected.

## References


Bhakta-Guha D and Efferth T (2015) Hormesis: decoding two sides of the same coin. *Pharmaceuticals (Basel)* **8**:865–883.

Calabrese EJ (2013) Hormetic mechanisms. *Crit Rev Toxicol* **43**:580–606.

Calabrese V, Giordano J, Ruggieri M, Berritta D, Trovato A, Ontario ML, Bianchini R, and Calabrese EJ (2016) Hormesis, cellular stress response, and redox homeostasis in autism spectrum disorders. *J Neurosci Res* **94**:1488–1498.

Cui T, Schopfer FJ, Zhang J, Chen K, Ichikawa T, Baker PR, Batthyany C, Chacko BK, Feng X, Patel RP, et al. (2006) Nitrated fatty acids: endogenous anti-inflammatory signaling mediators. *J Biol Chem* **281**:35686–35698.

Delmastro-Greenwood M, Freeman BA, and Wendell SG (2014) Redox-dependent anti-inflammatory signaling actions of unsaturated fatty acids. *Annu Rev Physiol* **76**:79–105.

Grgic I, Hofmeister AF, Genovese G, Bernhardy AJ, Sun H, Maarouf OH, Bijol V, Pollak MR, and Humphreys BD (2014) Discovery of new glomerular disease-relevant genes by translational profiling of podocytes in vivo. *Kidney Int* **86**: 1116–1129.

Hoerger TJ, Simpson SA, Yarnoff BO, Pavkov ME, Ríos Burrows N, Saydah SH, Williams DE, and Zhuo X (2015) The future burden of CKD in the United States: a simulation model for the CDC CKD Initiative. *Am J Kidney Dis* **65**:403–411.

Humphreys BD, Xu F, Sabbisetti V, Grgic I, Movahedi Naini S, Wang N, Chen G, Xiao S, Patel D, Henderson JM, et al. (2013) Chronic epithelial kidney injury molecule-1 expression causes murine kidney fibrosis. *J Clin Invest* **123**:4023–4035.

Jadhav A, Torlakovic E, and Ndisang JF (2008) Interaction among heme oxygenase, nuclear factor-kappaB, and transcription activating factors in cardiac hypertrophy in hypertension. *Hypertension* **52**:910–917.

Kadl A, Meher AK, Sharma PR, Lee MY, Doran AC, Johnstone SR, Elliott MR, Gruber F, Han J, Chen W, et al. (2010) Identification of a novel macrophage phenotype that develops in response to atherogenic phospholipids via Nrf2. *Circ Res* **107**:737–746.

Kansanen E, Bonacci G, Schopfer FJ, Kuosmanen SM, Tong KI, Leinonen H, Woodcock SR, Yamamoto M, Carlberg C, Ylä-Herttuala S, et al. (2011) Electrophilic nitro-fatty acids activate NRF2 by a KEAP1 cysteine 151-independent mechanism. *J Biol Chem* **286**:14019–14027.

Kansanen E, Jyrkkänen HK, Volger OL, Leinonen H, Kivelä AM, Häkkinen SK, Woodcock SR, Schopfer FJ, Horrevoets AJ, Ylä-Herttuala S, et al. (2009) Nrf2-dependent and -independent responses to nitro-fatty acids in human endothelial cells: identification of heat shock response as the major pathway activated by nitro-oleic acid. *J Biol Chem* **284**:33233–33241.

Kee HJ, Bae EH, Park S, Lee KE, Suh SH, Kim SW, and Jeong MH (2013) HDAC inhibition suppresses cardiac hypertrophy and fibrosis in DOCA-salt hypertensive rats via regulation of HDAC6/HDAC8 enzyme activity. *Kidney Blood Press Res* **37**: 229–239.

Kelley EE, Batthyany CI, Hundley NJ, Woodcock SR, Bonacci G, Del Rio JM, Schopfer FJ, Lancaster JR Jr, Freeman BA, and Tarpey MM (2008) Nitro-oleic acid, a novel and irreversible inhibitor of xanthine oxidoreductase. *J Biol Chem* **283**:36176–36184.

Liu Y, Jia Z, Liu S, Downton M, Liu G, Du Y, and Yang T (2013) Combined losartan and nitro-oleic acid remarkably improves diabetic nephropathy in mice. *Am J Physiol Renal Physiol* **305**:F1555–F1562.

Maher J and Yamamoto M (2010) The rise of antioxidant signaling–the evolution and hormetic actions of Nrf2. *Toxicol Appl Pharmacol* **244**:4–15.

Martini S, Nair V, Keller BJ, Eichinger F, Hawkins JJ, Randolph A, Böger CA, Gadegbeku CA, Fox CS, Cohen CD, et al.; European Renal cDNA Bank; C-PROBE Cohort; CKDGen Consortium (2014) Integrative biology identifies shared transcriptional networks in CKD. *J Am Soc Nephrol* **25**:2559–2572.

Nadkarni GN, Rao V, Ismail-Beigi F, Fonseca VA, Shah SV, Simonson MS, Cantley L, Devarajan P, Parikh CR, and Coca SG (2016) Association of urinary biomarkers of inflammation, injury, and fibrosis with renal function decline: the ACCORD trial. *Clin J Am Soc Nephrol* **11**:1343–1352.

Schopfer FJ, Vitturi DA, Jorkasky DK, and Freeman BA (2018) Nitro-fatty acids: new drug candidates for chronic inflammatory and fibrotic diseases. *Nitric Oxide* **79**: 31–37.

Tan SM, Sharma A, Stefanovic N, Yuen DY, Karagiannis TC, Meyer C, Ward KW, Cooper ME, and de Haan JB (2014) Derivative of bardoxolone methyl, dh404, in an inverse dose-dependent manner lessens diabetes-associated atherosclerosis and improves diabetic kidney disease. *Diabetes* **63**:3091–3103.

Verescakova H, Ambrozova G, Kubala L, Perecko T, Koudelka A, Vasicek O, Rudolph TK, Klinke A, Woodcock SR, Freeman BA, et al. (2017) Nitro-oleic acid regulates growth factor-induced differentiation of bone marrow-derived macrophages. *Free Radic Biol Med* **104**:10–19.

Vianna HR, Soares CM, Silveira KD, Elmiro GS, Mendes PM, de Sousa Tavares M, Teixeira MM, Miranda DM, and Simões E Silva AC (2013) Cytokines in chronic kidney disease: potential link of MCP-1 and dyslipidemia in glomerular diseases. *Pediatr Nephrol* **28**:463–469.

Villacorta L, Chang L, Salvatore SR, Ichikawa T, Zhang J, Petrovic-Djergovic D, Jia L, Carlsen H, Schopfer FJ, Freeman BA, et al. (2013) Electrophilic nitro-fatty acids inhibit vascular inflammation by disrupting LPS-dependent TLR4 signalling in lipid rafts. *Cardiovasc Res* **98**:116–124.

Villacorta L, Gao Z, Schopfer FJ, Freeman BA, and Chen YE (2016) Nitro-fatty acids in cardiovascular regulation and diseases: characteristics and molecular mechanisms. *Front Biosci* **21**:873–889.

Wang H, Liu H, Jia Z, Guan G, and Yang T (2010) Effects of endogenous PPAR agonist nitro-oleic acid on metabolic syndrome in obese zucker rats. *PPAR Res* **2010**:601562.

Wang H, Sun J, Jia Z, Yang T, Xu L, Zhao B, Yu K, and Wang R (2015) Nitrooleic acid attenuates lipid metabolic disorders and liver steatosis in DOCA-salt hypertensive mice. *PPAR Res* **2015**:480348.

Wang W, Li C, and Yang T (2016) Protection of nitro-fatty acid against kidney diseases. *Am J Physiol Renal Physiol* **310**:F697–F704.

Zoja C, Benigni A, and Remuzzi G (2014) The Nrf2 pathway in the progression of renal disease. *Nephrol Dial Transplant* **29** (Suppl 1):i19–i24.


**Address correspondence to:** Dr. Diane K. Jorkasky, Complexa, Inc., 1055 Westlakes Dr., Suite 200, Berwyn, PA 19312. E-mail: Diane.jorkasky@complexarx.com